Combining active and passive data for velocity reconstruction

J. Battaglia[1], D. Dello Iacono[2], A. Zollo[2], J. Virieux[3]

[1] *Laboratoire Magmas et Volcans, Université Blaise Pascal, CNRS, Clermont-Ferrand, France*

[2] *Dipartimento di Scienze Fisiche, Università degli Studi di Napoli Federico II, Napoli, Italy*

[3] *UMR Geosciences Azur, Sophia Antipolis, France*

Introduction

The Campi Flegrei caldera is situated west of the city of Naples in a highly populated area. It is assumed to be mostly the result of two explosive events: the Campanian Ignimbrite eruption (37 ka) and the Neapolitan Tuff eruption (12 ka) (Scandone et al., 1991; Orsi et al., 1996). The caldera is strongly affected by bradyseismic activity which is characterized by large scale vertical ground deformations. The two most recent episodes of large and rapid ground uplift, which occurred in 1970-72 and 1982-84, led to a cumulative maximum uplift of about 3.5 meters in the town of Pozzuoli (Orsi et al., 1999) and were accompanied by swarms of earthquakes and increased degassing.
The 1982-1984 bradyseismic crisis led to an uplift of about 1.8 meters (Barberi et al., 1984) and was accompanied by more than 15000 earthquakes. Part of this seismicity is used in the present tomographic study. The Campi Flegrei caldera has already been the target of several tomographic studies based on various sets of passive and active data. The different existing tomographic works provide various velocity models for Campi Flegrei depending on the data set and technique which was used. Our main goal in this paper is to provide a unique velocity model which satisfies both passive and active data sets: data from earthquakes recorded in 1984 as well as data from the more recent shots of the SERAPIS experiment. After presenting the different data sets which we use, we examine the effect of merging these sets which have very different characteristics and quantities. We then search for the optimal tomographic parameters and finally present the tomographic results and resolution tests.

Data

To obtain P and S velocity models of the Campi Flegrei caldera structure we proceed with a tomographic inversion based on travel times recorded during two distinct experiments (Figure 1). The first data set is composed of 606

earthquakes recorded during the end of the last bradiseismic crisis which occurred in 1982-1984. The events were recorded by a temporary digital network composed of 13 3-component stations which were installed by the University of Wisconsin, USA (UW) and by the 25 analog stations operated by the Osservatorio Vesuviano (OV) and AGIP. From the available events we selected a subset of 606 well constrained earthquakes with a minimum of 4 P travel times and 3 S travel times and an azimuthal gap in station coverage of less than 180 degrees. This passive data set provides a total of 4472 P and 3268 S travel times. The second data set is composed of recordings for 1528 shots produced during the SERAPIS experiment in September 2001. During the experiment were fired more than 5000 air-gun shots (Figure 1). To provide a high density of data in the bay of Pozzuoli, about 2500 shots were fired in the bay along E-W and N-S parallel lines 250 m apart with shots repeated every 125 m along each line. The shots were recorded with 154 stations, inclu-

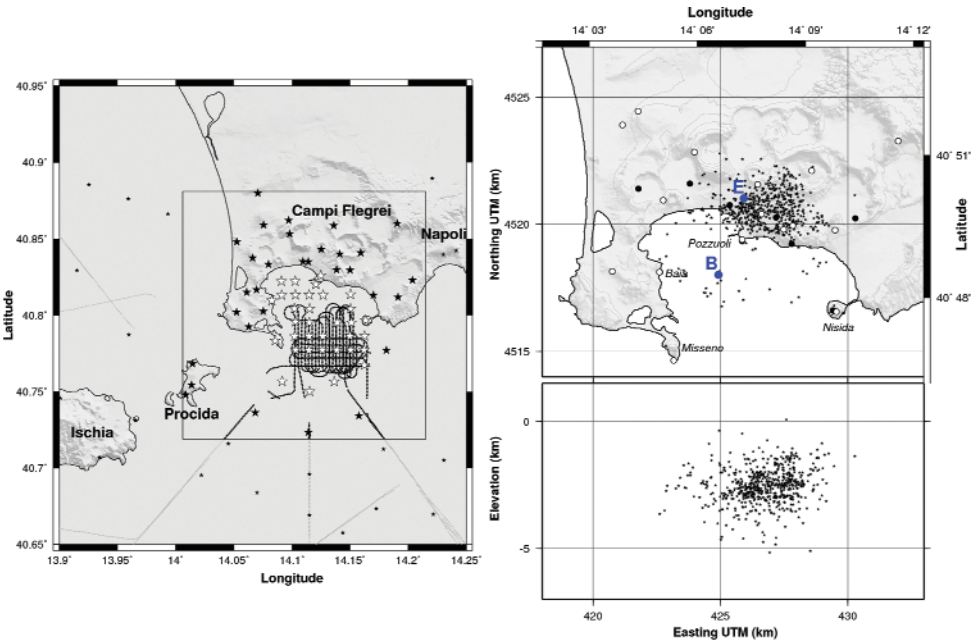

Fig. 1. Left: Shaded relief view of the Campi Flegrei caldera and Ischia and Procida islands with the tomography area in the center. The location of the shots used for tomography is indicated as black dots and the seismic stations are plotted as stars: empty stars for stations for which precisely re-picked arrival times are available and filled stars for stations for which only preliminary picks are available. The location of the shots outside the tomography area area and stations not used in the study is also indicated in lighter color. Right: hypocenters of 606 earthquakes recorded during the end of the 1982-1984 bradiseismic crisis and used in this study: map view and East-West cross-section below. The stations used for locating the events are shown as white circles for the stations of the temporary UW network and as black filled circles for the stations of the OV. Epicentral locations were spike tests have been performed to determined the effect of merging the data sets are indicated with blue dots.

ding 70 sea-bottom receivers (OBS three-component sensors) and 84 land stations (66 with 3-component sensors). The entire experiment produced a total of 700000 waveforms. In present work we only consider a subset of the entire available data set as we only use the shots and stations included in our tomographic area. Our active data set includes a total of 55123 travel times including 36195 re-picked (Dello Iacono et al. submitted) and 18928 picked travel times.

The tomographic inversion procedure

Three dimensional P and S velocity models are obtained by inverting P and S first arrival times simultaneously for both velocity models and earthquake locations (Thurber, 1992). The procedure is iterative and at each iteration a linearized inversion of delayed travel times is performed. The inversion is done with P and S velocity models parametrized as 3D grids of regularly spaced nodes. According to our station/source configuration, we consider a tomographic volume of 18*18*9 km starting 0.5 km above sea level (Figure 1) with a node spacing of 0.5 km in all directions. The forward problem of travel time computation is done by solving the Eikonal equation with a finite differences algorithm (Podvin and Lecomte, 1991). For this calculation we use fine P and S grids of constant slowness cells with a spacing of 0.1 km in all directions obtained by trilinear interpolation of the tomographic inversion grids. Travel time partial derivatives are computed simultaneously for P and S slowness fields, hypocenter locations and origin times of earthquakes (Le Meur et al., 1997). Normalization and scaling of the derivative matrix is performed to control the quality of the retrieved parameters. To ensure numerical stability and to control the degree of model roughness, the system is preconditioned and smoothed. The quality of the different observations is taken into account by weighting the different travel times. Finally, the inversion of the scaled and weighted linear system is done using the LSQR algorithm (Page and Saunders, 1982). The inversion is regularized using a damping factor.

Merging of the two sets of data

The joint inversion problem is made difficult since the passive and active data sets are complementary: the first one provides both Vp and Vs velocity models, as well as earthquake locations but has a lower resolution and a limited spatial coverage, while the second has a higher resolution but only provides P velocity and samples mostly shallow layers. Moreover the ray coverages provided by the two sets overlap only over a limited area and amounts of rays are very different. To examine the effect of merging the two data sets we made some spike tests at different epicentral locations and depths. Each spike test is

done by (1) adding to a smooth 1D initial velocity model a 500 m/s anomaly with a width of 1 km at half the pick amplitude, (2) calculating synthetic travel times for the chosen event/station configuration and (3) inverting the synthetic travel times starting from the original velocity model and using the same inversion parameters as for tomography. The tests emphasize that in areas where earthquakes are dominant, the joint inversion leads to a loss in resolution since spike reconstitution is lower than the one obtained when using only earthquakes. In areas dominated by shots the resolution remains unchanged when merging as compared to shots only, even if the resolution of the earthquakes is low (Figure 2). An adequate solution to compensate for the loss of resolution is to increase the weight of the earthquakes. Figure 3 shows

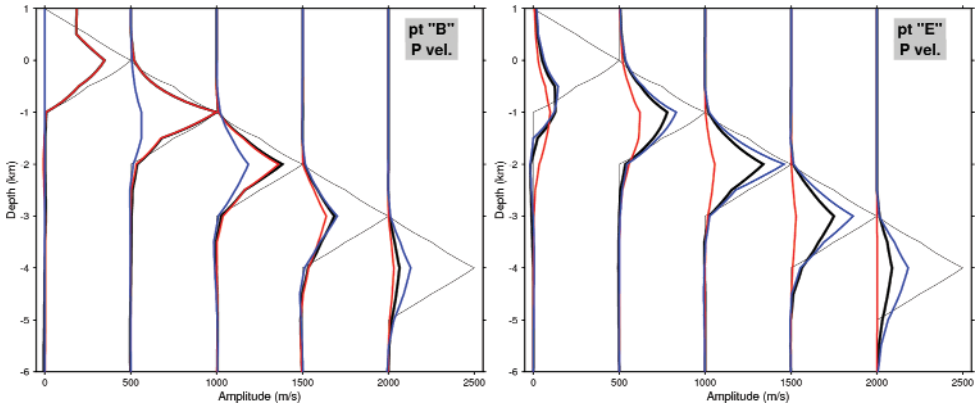

Fig. 2. Comparison between spike restitutions for P waves at points B and E when using shots only (red), earthquakes only (blue) and both (black).

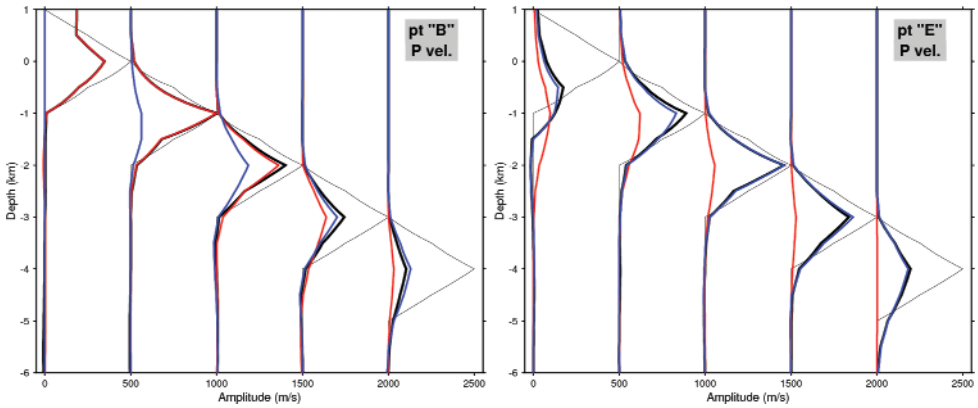

Fig. 3. Comparison between spike restitutions for P waves at points B and E when using shots only (red), earthquakes only (blue) and both with earthquakes weights multiplied by 2 (black).

a comparison of spike restitutions for three combinations of data: both shots and earthquakes alone and shots and earthquakes with the weight of earthquakes multiplied by a factor 2. However, we note that over-weighting the earthquakes using a factor higher than 2 has a negative effect on tomography as it can lead to unstable tomographic images. An alternate solution which allows to avoid the loss of resolution is to reduce the amounts of shots, but we note that it reduces the ability of reconstructing larger scale anomalies as shown later by doing larger scale "shape tests".

Inversion settings

To determine the optimal parameters to use in the tomography we perform synthetic tests in which larger scale velocity anomalies with various shapes are introduced ("shape tests"). We present here results for 2 different tests:

– Test T01: an annular anomaly with a 100 m/s amplitude added at each depth in the periphery of the tomography grid to the P velocity model.
– Test T02: a 100 m/s anomaly shaped as a cross added in the center of the grid at each depth to both P and S velocity models.

Figure 4 shows results obtained for tests T01 and T02 for various values of the damping and for various multiplicative factors applied to the weight of the earthquakes. Results suggest that appropriate values for Damping are in the range between 0.3 and 0.5. For P waves a good compromise is found in multiplying the weight of earthquakes by 2. To choose the proper S-wave multiplicative factor, we need to take into account another criterion which is the simplicity of the obtained velocity models when doing the tomography. It is well known that in tomography it is generally possible to find a whole class of models, which fits equally well the observations (Monteiller et al., 2006). The choice of the best model in that class is done by choosing the result with the lower degree of freedom (Akaike, 1974; Tarantola and Valette, 1982). For this purpose we examine the variance of the P and S velocity models and Vp/Vs ratio obtained with various multiplicative factors and examine the corresponding residuals for P and S travel times. Results indicate that a good choice is found with P-weights multiplied by 2 as suggested by above synthetic tests and S-weights multiplied by 2 or 4. The results for shape tests, performed by reducing the amounts of shots, indicate that it leads to a significant reduction in the ability to reproduce anomalies in the peripheral area of the grid where the resolution comes mostly from the shots. Results also indicate that the weight increase is only allowed by the stabilizing effect brought by the large amount of shots travel times. Finally, to determine a proper value to use for the smoothing coefficients we proceed with visual inspections of the recomposed anomalies. The images indicate that appropriate values for LX are in the range 0.2 to 0.3.

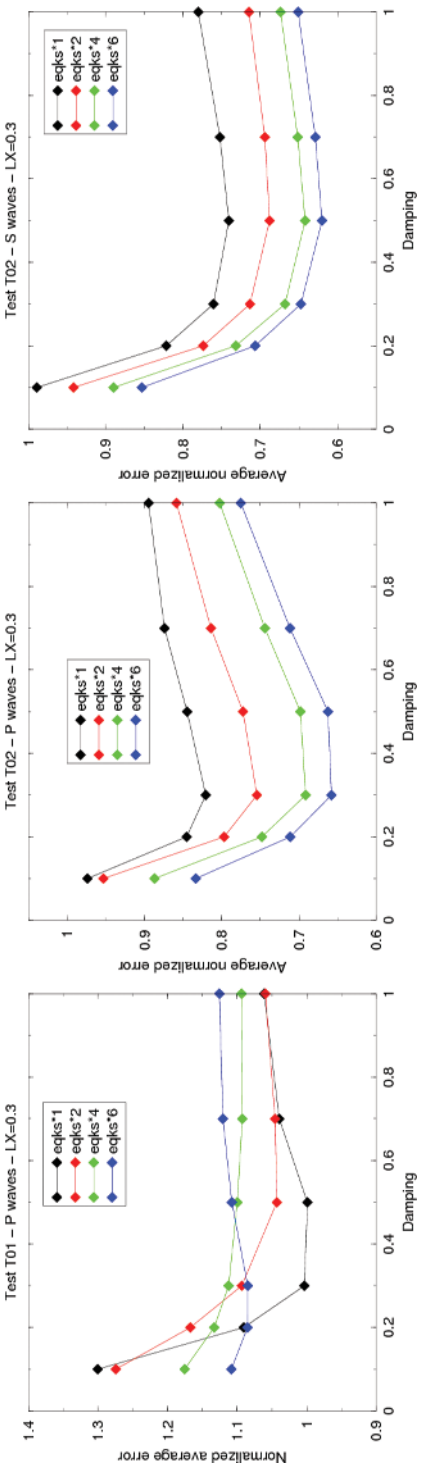

Fig. 4. Mean error rates for test T01 P waves and test T02 P and S waves as a function of the Damping. Each symbol represents the average of the absolute value of the difference between the introduced velocity anomaly and the one restored. This average is calculated over all nodes between 0 and 4 km b.s.l.

Tomography results

We present tomographic results obtained with DAMP=0.5, LX=0.3 and with the weight of earthquakes multiplied by 2 for both P and S waves. The tomography technique which we use is an iterative, linearized and perturbative technique. The choice of the initial 1D model was done in two steps. First, the 1D model chosen for Campi Flegrei caldera by Vanorio et al. (2005) was used as a starting model to process a first tomographic run. In a second time, the P and S resulting velocity models were used to calculate average vertical velocity profiles for both P and S waves. The obtained profiles are used as initial models. The iterative process is stopped after 15 iterations, while most of the rms residual reduction is achieved in the first five iterations. The process drops the rms from about 0.15 to 0.07.
The obtained 3D velocity models, as well as earthquakes locations are shown in Figures 5 and 6. The obtained high resolution tomographic images outline 3 major features: 1/ The P velocity model (Figure 5) confirms the presence of

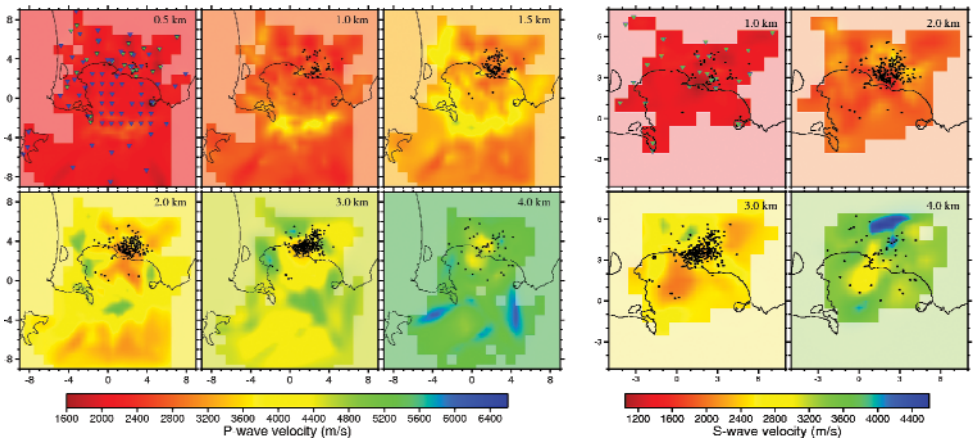

Fig. 5. Tomography results: (left) horizontal sections of the P velocity model. (right) horizontal sections of the S velocity model. Cells not sampled by any ray are shown in lighter colors.

a high P velocity ring in the southern part of the bay of Pozzuoli and extends its trace inland as compared to previous results. 2/ The Vp/Vs East-West cross section at y=2500 (Figure 6), which passes below the town of Pozzuoli, outlines the presence of a very high Vp/Vs anomaly located below the town of Pozzuoli. 3/ Horizontal cross-sections of the Vp/Vs ratio (Figure 6) confirm the presence of a low Vp/Vs body extending at about 4 km depth below a large part of the caldera

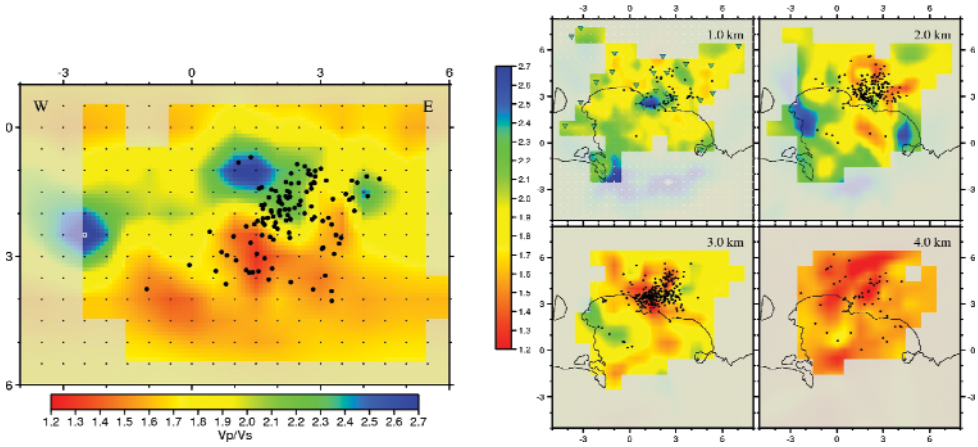

Fig. 6. Tomography results: (left) East-West cross-section at y=2500 of the Vp/Vs ratio; (right) horizontal cross-sections of the Vp/Vs ratio.

Resolution tests

To identify the well resolved areas of the tomographic images, we made several synthetic tests including a checkerboard test with 2 km cells with a +/-100 m/s amplitude and several shape tests (Figures 7 and 8). Those are done in a similar way as the tests used to determine proper inversion parameters except that in the present case the position of the earthquake sources are fixed. The checkerboard test indicates an optimal resolution for P waves at 1.5 km b.s.l. below a large part of the tomography grid. For S waves a good resolution is obtained below and around the town of Pozzuoli from about 1.5 to 3.5 km b.s.l.. The shape test in Figure 8 indicates a good restitution of an annular anomaly added to the P velocity model in the periphery of the tomography grid down to 2-3 km b.s.l.. A good reproduction of Vp/Vs anomalies is also obtained below the Pozzuoli area.

Conclusion and discussion

We show that by properly weighting the different data sets we are able to retrieve optimally the information provided individually by each set. The merging of the two types of data provides a single set of P and S velocity models which satisfy simultaneously all available data. Previous results obtained from gravimetric, seismic activity, and drilled-rock sampling analyses conducted in Pozzuoli Gulf and on land have been used for geological interpretation of Vp and Vp/Vs anomalies.

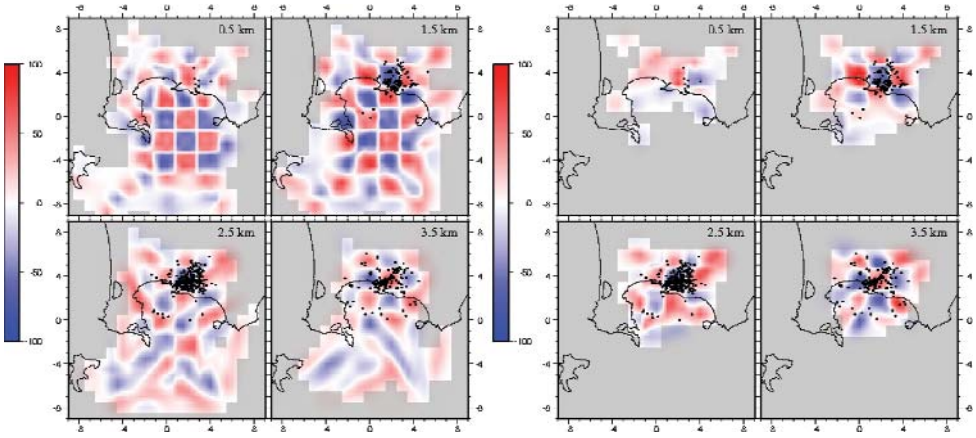

Fig. 7. Results for a checkerboard test with 2*2*2 km cells with +/- 50m/s anomalies added to P (left) and S (right) velocities.

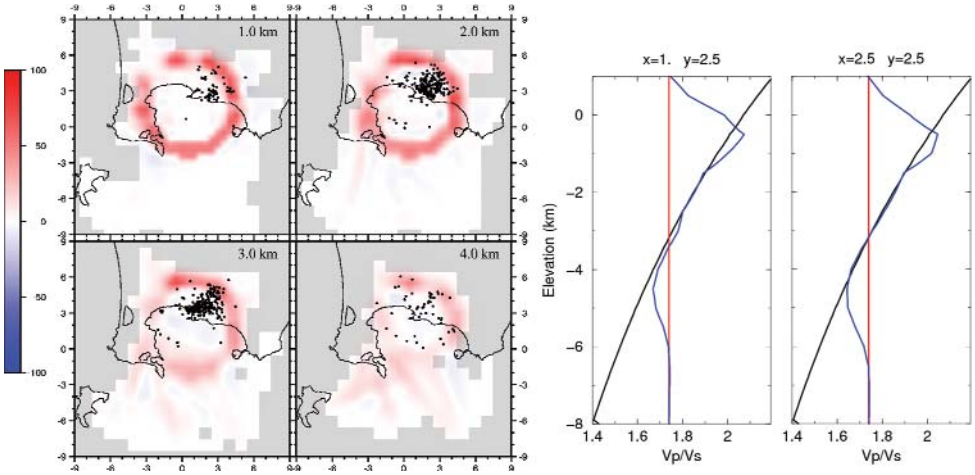

Fig. 8. Results for synthetic T01b showing the reconstruction of the P anomaly at different depths (left) and 2 vertical profiles showing the reconstruction (blue) of the Vp/Vs anomaly (black).

By analysing the horizontal sections of the P-velocity model (Figure 5) we observe at about 1.5 km depth an arc-like positive anomaly with a diameter of about 10 km and a width of about 1 km which is interpreted as the buried trace of the caldera rim (Zollo et al., 2003; Judenherc and Zollo, 2004). By comparing the tomographic image with Bouguer anomaly maps, based on data acquired in early eighties (Agip, 1987; Barberi et al., 1991, Florio et al., 1999; Capuano and Achauer, 2003) one can find a good correlation between the

geometry and position of the velocity anomaly and the positive gravity anomaly, which has been attributed to the presence of hydrothermalized lava formations. At approximately the same depth an anomalous high value of the Vp/Vs ratio is observed in the central area of the caldera on the vertical cross-section passing below the town of Pozzuoli (Figure 6). This anomaly may be the evidence for a thick brine rock sedimentary layer (Vanorio et al., 2005). Recently Dello Iacono et al. (submitted), by analysing the P-to-P and P-to-S reflected phases, extended the area of abnormally high Vp/Vs ratio observed in the first 500/700 m to the entire bay of Pozzuoli and interpreted this result as a consequence of the presence of incoherent, water saturated, volcanic and marine sediments.

Overall, The Campi Flegrei caldera appears as a sub-circular shape with a height of about 2 km. Because of the strong lateral heterogeneity, the caldera border acts like a strong scatterer for seismic waves (Tramelli et al., 2006). At about 4 km depth the annular Vp anomaly disappears. The tomographic Vp velocities of 5500 m/s found at that depth are compatible with those of carbonatic rocks which likely form the deep basement of the caldera (Judenherc and Zollo, 2004). At the same depth, the horizontal crosssections of the Vp/Vs ratio confirm the presence of a low Vp/Vs body extending below a large part of the caldera (Vanorio et al., 2005; Chiarabba and Moretti, 2007). Earthquakes are located at the top of this anomaly. According to the dependence of Vp and Vs velocities to fluid saturation and the interpretation of Vanorio et al. (2005), we believe that the low Vp/Vs value at 4 km depth excludes the presence of melted rocks and is due to the presence of overpressured gas-bearing fractured formations.

Acknowledgments

This work has been partially funded by the SPICE project (Contract Number MRTN-CT2003-504267) of the European Commission's Human Resources and Mobility Programme.

References

Akaike, H., 1974. A new look at the statistical model identification. IEEE Trans. Autom. Contr., 19 (6), 716-723.

Barberi, F., Corrado, G., Innocenti, F., Luongo, G., 1984. Phlegrean Fields 1982-1984: Brief chronicle of a volcano emergency in a densely populated area. Bull. Volcanol., 47 (2), 175-185.

Barberi, F., Cassano, E., La Torre, P., Sbrana, A., 1991. Structural evolution of Campi Flegrei caldera in light of volcanological and geophysical data. J. Volcanol. Geotherm. Res. 48, 33-49.

Capuano P., Achauer U. 2003. Gravity field modeling in the Vesuvius and Campanian area. TomoVes Seismic Project: Looking Inside Mt. Vesuvius, edited by A. Zollo et al., Cuen, Napoli, 2003

Chiarabba C. and Moretti M. 2006. An insight into the unrest phenomena at the Campi Flegrei caldera from Vp and Vp/Vs tomography. Terra Nova, 18, 373-379.

Dello Iacono D., Zollo A., Vassallo M., Vanorio T., Judenherc S. 2007. Seismic images and rock properties of the very shallow structure of Campi Flegrei caldera (southern Italy). Submitted

Florio G., Fedi M., Cella F., Rapolla A., 1999. The Campanian Plain and Campi Flegrei: structural setting from potential field data. J. Volcanol. Geotherm. Res., 91, 361-379.

Judenherc S. and Zollo A. 2004. The Bay of Naples (Southern Italy): constraints on the volcanic structures inferred from a dense seismic survey. J. Geophys. Res. 109, B10312.

Le Meur, H., J. Virieux, and P. Podvin (1997), Seismic tomography of the Gulf of Corinth: A comparison of methods, Ann. Geophys, 40, 1-25.

Monteiller V. 2005. Tomographie à l'aide de décalages temporels d'ondes sismiques P: développements méthodologiques et applications, Thèse de Doctorat, Université de Savoie.

Orsi, G., de Vita, S., Di Vito, M., 1996. The restless, resurgent Campi Flegrei nested caldera (Italy): constraints on its evolution and configuration. J. Volcanol. Geotherm. Res., 74, 179-214.

Orsi, G., Civetta, L., Del Gaudio, C., de Vita, S., Di Vito, M.A., Isaia, R., Petrazzuoli, S.M., Ricciardi, G.P., Ricco, C., 1999. Short-term ground deformations and seismicity in the resurgent

Campi Flegrei caldera (Italy): An example of active block-resurgence in a densely populated area. J. Volcanol. Geotherm. Res., 91, 415-451.

Paige, C. C., and M. A. Saunders, 1982. LSQR: An algorithm for sparse linear equations and sparse least squares, Trans. Math. Software, 8, 43-71.

Podvin, P., and I. Lecomte, 1991. Finite difference computation of traveltimes in very contrasted velocity models: A massively parallel approach and its associated tools, Geophys. J. Int., 105, 271-284.

Scandone, R., Bellucci, F., Lirer, L., Rolandi, G., 1991. The structure of the Campanian plain and the activity of the Napolitan volcanoes. J. Volcanol. Geotherm. Res., 48, 1-31.

Tarantola, A., and B. Valette, 1982. Generalized nonlinear inverse problems solved using the least-squares criterion, Rev. Geophys., 20, 219-232.

Tramelli A., Del Pezzo E., Bianco F. and Boschi E., 2006. 3D scattering image of the Campi Flegrei caldera (Southern Italy). Phys. Earth Planet. Inter. 155, 3-4, 269-280.

Thurber, C. H., 1992. Hypocenter-velocity structure coupling in local earthquake tomography, Phys. Earth Planet. Inter., 75, 55-62.

Vanorio T., Virieux J., Capuano P. and Russo G., 2005. Three-dimensional seismic tomography from P wave and S wave microearthquake travel times and rock physics characterization of the Campi Flegrei Caldera. J. Geophys. Res. 110, B03201, doi:10.1029/2004GL003102.

Zollo, A., et al., 2003. Evidence for the buried rim of Campi Flegrei caldera from 3-d active seismic imaging, Geophys. Res. Lett., 30(19), 2002, doi:10.1029/2003GL018173.